Inorganic Chemistry

pubs.acs.org/IC

Communication

Insight into the Maturation Process of the Nitrile Hydratase Active Site

Irene R. A. M. Ogutu, Richard C. Holz,* and Brian Bennett*

Cite This: *Inorg. Chem.* 2021, 60, 5432−5435

Read Online

ACCESS | Metrics & More | Article Recommendations | Supporting Information

ABSTRACT: The metal binding motif of all nitrile hydratases (NHases, EC 4.2.1.84) is highly conserved (CXXCSCX) in the α-subunit. Accordingly, an eight amino acid peptide (VCTLCSCY), based on the metal binding motif of the Co-type NHase from *Pseudonocardia thermophilia* (*Pt*NHase), was synthesized and shown to coordinate Fe(II) under anaerobic conditions. Parallel-mode EPR data on the mononuclear Fe(II)−peptide complex confirmed an integer-spin signal at $g' \sim 9$, indicating an $S = 2$ system with unusually small axial ZFS, $D = 0.29$ cm^{-1} Exposure to air yielded a transient high-spin EPR signal most consistent with an intermediate/admixed $S = {}^3/_2$ spin state, while the integer-spin signal was extinguished. Prolonged exposure to air resulted in the observation of EPR signals at $g = 2.04$, 2.16, and 2.20, consistent with the formation of a low-spin Fe(III)−peptide complex with electronic and structural similarity to the NHase from *Rhodococcus equi* TG328−2 (*Re*NHase). Coupled with MS data, these data support a progression for iron oxidation in NHases that proceeds from a reduced high spin to an oxidized high spin followed by formation of an oxidized low-spin iron center, something that heretofore has not been observed.

Nitrile hydratases (NHases, EC 4.2.1.84) are metalloenzymes that contain either a nonheme low-spin Fe(III) ion (Fe-type) or a noncorrin low-spin Co(III) ion (Co-type) in their active site.[1−4] NHases have proven useful as biocatalysts in preparative organic chemistry and the industrial production of acrylamide and nicotinamide.[5] They have also been used in the bioremediation of nitrile-based chemicals and pesticides such as bromoxynil and are thus recognized as "Green" catalysts.[6] In both Fe- and Co-type NHases, the metal ions are six-coordinate and bound by a labile water, three cysteines, and two backbone amide nitrogen's that are deprotonated with significant double bond character in the CN bond.[7] Interestingly, two of the active site cysteine residues are post-translationally modified to cysteine−sulfinic acid (−SO_2H) and cysteine−sulfenic acid (−SOH), yielding an unusual metal coordination geometry that was termed a "claw-setting". It has been shown that unless this Cys oxidation process occurs, NHase is inactive, consistent with the sulfenic acid ligand acting as the nucleophile during catalytic turnover.[8,9] While an activator protein has been implicated in inserting a divalent metal ion into the α-subunit,[10,11] little is known regarding how the controlled oxidation of the active site metal ion and the two equatorial Cys residues occur, as it happens *in vivo*, to produce the required active site architecture.[12]

We recognized that the NHase metal binding motif (CXXCSCX), which is ubiquitous among NHases,[7,13] contains all of the active site ligands in an eight amino acid sequence and hypothesized that such a peptide could bind Fe(II) forming a biomimetic NHase complex.[3,24,2528] An eight amino acid peptide (VCTLCSCY), based on the metal binding motif of the Co-type NHase from *Pseudonocardia thermophilia* (*Pt*NHase), was synthesized (GenScript) (Figure 1) with an acetyl group attached to the N-terminal to enhance solubility

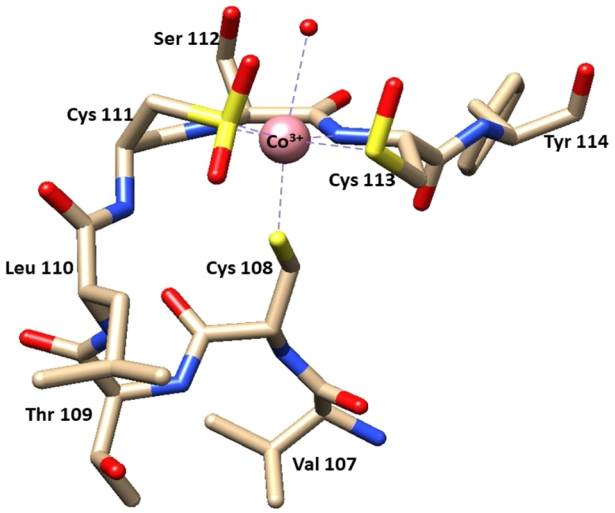

Figure 1. Active site of the Co-type NHase from Pseudonocardia thermophilia (PtNHase) based on the X-ray crystal structure (PDB: 1IRE)[14] showing eight of the amino acid residues that make up the peptide VCTLCSCY.

(Figure 2I). As the active site is ubiquitous among both Co- and Fe-type NHases, we chose to titrate Fe(II) into this peptide in 10 mM NEM buffer pH 8.0 under anerobic

Received: October 1, 2020
Published: March 29, 2021

https://doi.org/10.1021/acs.inorgchem.0c02924
Inorg. Chem. 2021, 60, 5432−5435

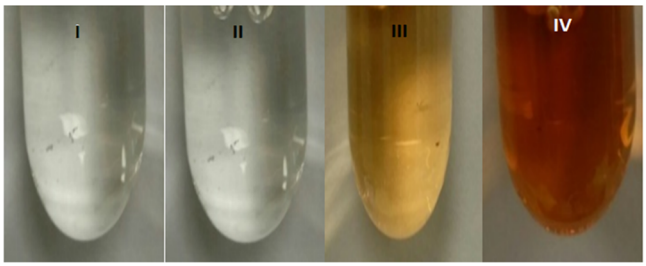

Figure 2. 0.76 mM PtNHase peptide solution in 10 mM NEM buffer pH 8.0 at 25 C under anaerobic conditions. (i) PtNHase peptide solution with no metal, (ii) Fe(II)-bound PtNHase peptide complex, (iii) oxidized Fe-bound PtNHase peptide complex after exposure to air for 5 min, and (iv) oxidized Fe-bound PtNHase peptide complex after exposure to air for 3 h.

conditions, which provided a colorless solution (Figure 2II). Upon exposure to air, the solution turned light orange and over time and intensified to an orange-brown color (Figure 2III,IV). UV−vis spectra exibited an absorption band at 490 nm with a shoulder at ∼435 nm (Table S1 and Figure S1). These bands are characteristic of S-to-Fe(III) LMCT bands[15] and are similar to those observed for the Fe-type NHases from *Rhodococcus equi* TG328-2 (*Re*NHase).[16] However, the characteristic axial S-to-Fe(III) LMCT band at ∼700 nm observed for Fe-type NHases was absent for the Fe(III)-bound peptide model complex.[16] These data indicate ligation of Fe(II) to the cysteine residues of the peptide followed by oxidation to Fe(III).

The electronic and structural aspects of the observed iron oxidation process were further investigated by X-band EPR of the anaerobically prepared Fe(II)−peptide complex (Figure 3,

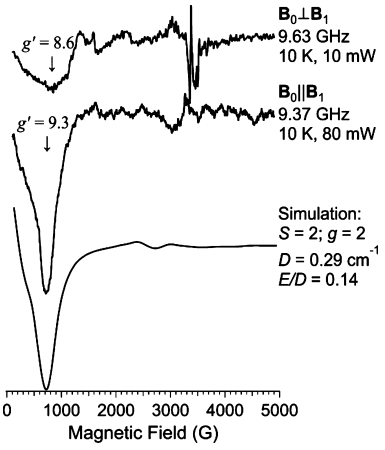

Figure 3. EPR spectra of a 0.76 mM Fe(II)-bound PtNHase peptide complex in 10 mM NEM buffer, pH 8.0, under anaerobic conditions. The top two traces show the perpendicular- and parallel-mode EPR spectra, respectively, while the bottom trace is a computer simulation invoking an $S = 2$ system with a zero-field splitting envelope that is partially accessible by the microwave quantum (9.37 GHz).

top trace). In perpendicular mode ($\mathbf{B}_0 \perp \mathbf{B}_1$), the signal exhibited no immediately assignable features except an ill-defined low-field trough extending from zero-field to around 1200 G, with a minimum at $g' \sim 9$. EPR spectra recorded in parallel-mode ($\mathbf{B}_0 \| \mathbf{B}_1$) yielded an intense resonance at $g' \sim 9$ (Figure 3, middle), suggesting an $S = 2$ system by virtue of the $g' \approx 4S$ rule.[17] The signal disappears into zero-field because the envelope of zero-field splitting energies extends beyond the microwave quantum energy and, additionally, a signal from only one non-Kramers doublet is observed, so the spin Hamiltonian parameters are not uniquely determinable.[17] However, a good simulation was obtained (Figure 3, bottom) using $S = 2$, $g = 2$, and a zero-field splitting envelope with $D = 0.29$ cm^{-1}, $E/D = 0.14$, $\sigma D = 1.2$ GHz, and $\sigma E = 200$ MHz, consistent with high-spin Fe(II) with octahedral coordination.

After exposure to air for 3 h. the integer-spin signal was diminished by a factor of 3 and an intense high-spin half-integer signal was observed with overlapping low-field peaks at $g' = 6.0$ and $g' = 5.2$ (Figure 4). No signals were observed at

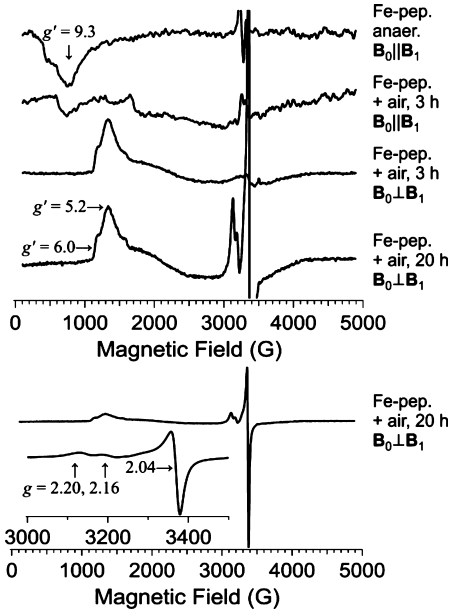

Figure 4. EPR spectra of a 0.76 mM Fe-bound PtNHase peptide complex in 10 mM NEM buffer, pH 8.0. Top panel: The top two traces show the parallel-mode EPR spectra (10 K, 80 mW, 9.37 GHz) under anaerobic conditions (top) and after 3 h exposure to air (bottom). The bottom two traces show the corresponding perpendicular-mode spectra (10 K, 10 mW, 9.63 GHz) sample exposed to air for 3 and 20 h, respectively. Bottom panel: The main trace shows the entire spectrum of the Fe-bound PtNHase peptide complex exposed to air for 20 h (inset: $g \sim 2$ region).

resonant fields corresponding to $g > 6$, and there was no evidence to suggest that the $g' = 6.0$ resonance was a derivative-like feature rather than a peak. The signal also exhibited a broad "S"-shaped absorption from 1600 to 4300 G, suggestive of a rhombic signal with $g_2' \approx 3.3$ and $g_3' < 2$, in addition to the prominent $g_1' = 5.2$ signal. That ensemble of resonances is inconsistent with the expected $S = {}^5/_2$ spin system but is entirely consistent with the $M_S = \pm{}^1/_2$ doublet of an $S = {}^3/_2$ spin system. In addition, the sharp resonance and cutoff of absorption at $g' = 6.0$ are expected for an $M_S = \pm{}^1/_2$, $S = {}^3/_2$ signal with $g_{real} = 2$ and a line shape determined by strains in the rhombic zero-field splitting parameter, E/D; an analogous phenomenon is observed for rhombic ($E/D > 0$) high-spin Fe(III) at $g' = \sim 10$.[18]

Intermediate spin (IS) or admixed spin $S = {}^3/_2$ Fe(III) is unusual and its appearance warrants some scrutiny. Occurrences are most common in porphyrin systems with significant deviations from planarity, and the signal reported herein closely resembles that of a substituted Fe−porphyrin complex

https://doi.org/10.1021/acs.inorgchem.0c02924
Inorg. Chem. 2021, 60, 5432−5435

reported by Yatsunyk and Walker.[19] In that case, the signal was assigned to an Fe(II)−porphyrinate radical antiferromagnetic charge-transfer complex. However, simpler mononuclear Fe(III) IS complexes have been studied and the $S = {}^3/_2$ state of the Fe(III) ion substantiated with *ab initio* density functional theoretical (DFT) calculations and structural characterization,[20] including for a functional mimic of hydrogenase.[21] This latter study indicated that the spin state was a determinant of the structure of the biomimetic model and may influence its chemical reactivity. Other possible explanations for the signal are (i) an Fe(II)−protein radical complex, (ii) a high-spin {FeNO}^{7} complex, and (iii) Co(II), which can be elimiated on the basis of metal analysis data. Nitric oxide can also be eliminated as there is no source of it in the Fe−peptide system. Finally, no highly reducing or oxidizing conditions were employed that would likely result in radical formation.

Exposure of the Fe−peptide complex to air for ∼20 h revealed that the high-spin Fe(III) signal persisted, retaining ∼90% intensity, consistent with the observed UV−vis spectra; however, an additional signal with high amplitude was observed in the $g \sim 2$ region. This latter signal was characterized as an axial $g\perp$ resonance at $g = 2.04$ and two distinct $g\|$ resonances at $g = 2.20$ and 2.16, respectively. These EPR parameters can be compared to those reported for active *Re*NHase with a bound water molecule (*Re*NHase^{Aq}), which exhibits *g*-values of 2.20, 2.13, and 1.99,[22,23] and with those from model compounds that exhibit *g*-values within the range $2.3 > g > 1.97$.[24] Despite the very high amplitude of these low-spin Fe(III) peptide complex EPR signals, their contribution to the total spin density was ∼5%.

In conclusion, the spectroscopic data reported coupled with MALDI-TOF MS data (Table S1; Figures S2 and S3) provides insight into a heretofore unknown iron maturation process for NHase active sites (Scheme 1). The formation of a colorless solution (**1**) upon the addition of Fe(II) to the peptide is associated with an $S = 2$ integer-spin signal from a mononuclear Fe(II) complex that MS data verify as the fully reduced peptide. Oxidation of Fe(II) to Fe(III) upon exposure to air is indicated by development of a straw colored sample and by EPR data, as the integer-spin signal due to Fe(II) slowly diminishes and is replaced by signals consistent with the formation of an $S = {}^3/_2$ intermediate-spin Fe(III) peptide complex (**2**) that MS data confirm is a mixture of fully reduced and singly oxidized peptide. These data suggest that the first step in the NHase maturation process is likely oxidation of the active site iron center. After exposure to air for 20 h, MS data reveal that both fully reduced peptide (**2**) and singly oxidized peptide (**3**) remain the prevalent forms. There is no evidence for an $S = {}^5/_2$ signal and therefore iron is likely still in the $S = {}^3/_2$ state. However, MS data also suggest small amounts of both doubly oxidized (**4**) and triply oxidized (**5**) peptides.[25] The presence of a small amount of (**5**) is also suggested by the $S = {}^1/_2$ EPR signal. The signal exhibits *g*-values that are comparable to those from *Re*NHase^{Aq}.[23] A recent study suggests that Fe(II) is initially inserted onto the NHase active site by the activator protein[10] and that once high-spin Fe(II) is bound to the NHase active site, oxidation to a high-spin Fe(III) center with concomitent stepwise oxidation of the equatorial Cys residues to sulfinic and sulfenic acids occurs,[12] until a low-spin Fe(III) center is formed. Nevertheless, the possibility remains that, in the peptide system, the $S = {}^1/_2$ EPR signal could arise from either species **4a**, **4b**, or **5**, although available evidence favors species **5** as the source of at least one of the $S = {}^1/_2$ signals.

Scheme 1. Proposed Progression of Iron Oxidation in NHases That Proceeds through Reduced High-Spin (1) → Oxidized High-Spin (2, 3, & 4) → Oxidized Low-Spin (5) Iron Centers

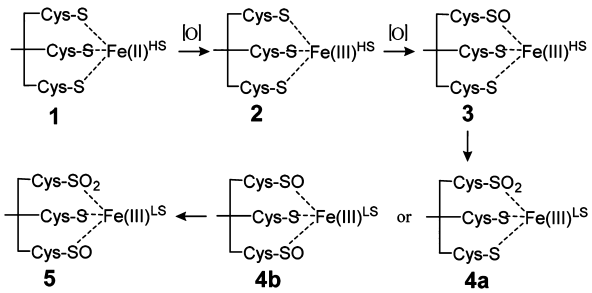

■ ASSOCIATED CONTENT

Supporting Information

The Supporting Information is available free of charge at https://pubs.acs.org/doi/10.1021/acs.inorgchem.0c02924.

Detailed description of the materials and methods, tables of UV−vis data and possible MALDI-TOF peaks, and UV−vis and MALDI-TOF spectra (PDF)

■ AUTHOR INFORMATION

Corresponding Authors

Richard C. Holz − *Department of Chemistry, Colorado School of Mines, Golden, Colorado 80401, United States; Department of Chemistry, Marquette University, Milwaukee, Wisconsin 53201-1881, United States;* orcid.org/0000-0001-6093-2799; Phone: (303) 273-3003; Email: rholz@mines.edu

Brian Bennett − *Department of Physics, Marquette University, Milwaukee, Wisconsin 53233, United States;* orcid.org/0000-0003-2688-1478; Phone: (414) 288-6705; Email: brian.bennett@marquette.edu

Author

Irene R. A. M. Ogutu − *Department of Chemistry, Colorado School of Mines, Golden, Colorado 80401, United States; Department of Chemistry, Marquette University, Milwaukee, Wisconsin 53201-1881, United States*

Complete contact information is available at: https://pubs.acs.org/10.1021/acs.inorgchem.0c02924

Notes

The authors declare no competing financial interest.

■ ACKNOWLEDGMENTS

This work was supported by the National Science Foundation (CHE-2003861, RCH; CHE-1808711, RCH & BB; CHE-1308672, BB; CHE-1532168 BB & RCH), the Todd Wehr Foundation, Bruker Biospin, and the National Institutes of Health/NIBIB National Biomedical EPR Center (P41-EB001980).

https://doi.org/10.1021/acs.inorgchem.0c02924
Inorg. Chem. 2021, 60, 5432−5435

REFERENCES

(1) Banerjee, A.; Sharma, R.; Banerjee, U. C. The nitrile-degrading enzymes: current status and future prospects. *Appl. Microbiol. Biotechnol.* **2002**, *60*, 33−44.

(2) Endo, I.; Nojiri, M.; Tsujimura, M.; Nakasako, M.; Nagashima, S.; Yohda, M.; Odaka, M. Fe-type nitrile hydratase. *J. Inorg. Biochem.* **2001**, *83*, 247−253.

(3) Kovacs, J. A. Synthetic analogues of cysteinate-ligated non-heme iron and non-corrinoid cobalt enzymes. *Chem. Rev.* **2004**, *104*, 825−848.

(4) Harrop, T. C.; Mascharak, P. K. Fe(III) and Co(III) centers with carboxamido nitrogen and modified sulfur coordination: lessons learned from nitrile hydratase. *Acc. Chem. Res.* **2004**, *37*, 253−260.

(5) Mathew, C.; Nagasawa, T.; Kobayashi, M.; Yamada, H. Nitrilase catalyzed production of nicotinic acid from 3-cyanopyridine in Rhodococcus rhodochrous J1. *Appl. Environ. Microbiol.* **1988**, *54*, 1030−1032.

(6) Baxter, J.; Cummings, S. P. The current and future applications of microorganism in the bioremediation of cyanide contamination. *Antonie van Leeuwenhoek* **2006**, *90*, 1−17.

(7) Miyanaga, A.; Fushinobu, S.; Ito, K.; Wakagi, T. Crystal structure of cobalt-containing nitrile hydratase. *Biochem. Biophys. Res. Commun.* **2001**, *288* (5), 1169−1174.

(8) Tsujimura, M.; Odaka, M.; Nakayama, H.; Dohmae, N.; Koshino, H.; Asami, T.; Hoshino, M.; Takio, K.; Yoshida, S.; Maeda, M.; Endo, I. A novel inhibitor for Fe-type nitrile hydratase: 2-cyano-2-propyl hydroperoxide. *J. Am. Chem. Soc.* **2003**, *125*, 11532−11538.

(9) Dey, A.; Chow, M.; Taniguchi, K.; Lugo-Mas, P.; Davin, S.; Maeda, M.; Kovacs, J. A.; Odaka, M.; Hodgson, K. O.; Hedman, B.; Solomon, E. I. Sulfur K-Edge XAS and DFT Calculations on Nitrile Hydratase: Geometric and Electronic Structure of the Non-heme Iron Active Site. *J. Am. Chem. Soc.* **2006**, *128*, 533−541.

(10) Lankathilaka, K. P. W.; Bennett, B.; Holz, R. C. The Fe-type nitrile hydratase from Rhodococcus equi TG328−2 forms an alpha-activator protein complex. *JBIC, J. Biol. Inorg. Chem.* **2020**, *25*, 903−911.

(11) Zhou, Z.; Hashimoto, Y.; Shiraki, K.; Kobayashi, M. Discovery of posttranslational maturation by self-subunit swapping. *Proc. Natl. Acad. Sci. U. S. A.* **2008**, *105*, 14849−14854.

(12) Arakawa, T.; Kawano, Y.; Katayama, Y.; Nakayama, H.; Dohmae, N.; Yohda, M.; Odaka, M. Structural Basis for Catalytic Activation of Thiocyanate Hydrolase Involving Metal-Ligated Cysteine Modification. *J. Am. Chem. Soc.* **2009**, *131* (41), 14838−14843.

(13) Nishiyama, M.; Horinouchi, S.; Kobayashi, M.; Nagasawa, T.; Yamada, H.; Beppu, T. Cloning and characterization of genes responsible for metabolism of nitrile compounds from Pseudomonas chlororaphis B23. *J. Bacteriol.* **1991**, *173* (8), 2465−72.

(14) Miyanaga, A.; Fushinobu, S.; Ito, K.; Wakagi, T. Crystal structure of cobalt-containing nitrile hydratase. *Biochem. Biophys. Res. Commun.* **2001**, *288*, 1169−1174.

(15) Kennepohl, P.; Neese, F.; Schweitzer, D.; Jackson, H. L.; Kovacs, J. A.; Solomon, E. I. Spectroscopy of non-heme iron thiolate complexes: Insight into the electronic structure of the low-spin active site of nitrile hydratase. *Inorg. Chem.* **2005**, *44* (6), 1826−1836.

(16) Gumataotao, N.; Kuhn, M. L.; Hajnas, N.; Holz, R. C. Identification of an active site-bound nitrile hydratase intermediate through single turnover stopped-flow spectroscopy. *J. Biol. Chem.* **2013**, *288* (22), 15532−6.

(17) Hagen, W. R. EPR Spectroscopy of Iron-Sulfur Proteins. 1992, 38, 165−222. *Adv. Inorg. Chem.* **1992**, *38*, 165−222.

(18) Copik, A. J.; Waterson, S.; Swierczek, S. I.; Bennett, B.; Holz, R. C. Both Nucleophile and Substrate Bind to the Catalytic Fe(II)-Center in the Type-II Methionyl Aminopeptidase from Pyrococcus furiosus. *Inorg. Chem.* **2005**, *44*, 1160−1162.

(19) Yatsunyk, L. A.; Walker, F. A. Structural, NMR, and EPR Studies of S = 1/2 and S = 3/2 Fe(III) Bis(4-Cyanopyridine) Complexes of Dodecasubstituted Porphyrins. *Inorg. Chem.* **2004**, *43*, 757−777.

(20) Chowdhury, S. R.; Mishraa, S. Ab initio investigation of magnetic anisotropy in intermediate spin iron(iii) complexes. *J. Chem. Phys.* **2018**, *149*, 234302.

(21) Edler, E.; Stein, M. Spin-State-Dependent Properties of an Iron(III) Hydrogenase Mimic. *Eur. J. Inorg. Chem.* **2014**, *2014* (22), 3587−3599.

(22) Lankathilaka, K. P. W.; Stein, N.; Holz, R. C.; Bennett, B. Cellular maturation of an iron-type nitrile hydratase interrogated using EPR spectroscopy. *JBIC, J. Biol. Inorg. Chem.* **2019**, *24* (7), 1105−1113.

(23) Stein, N.; Gumataotao, N.; Hajnas, N.; Wu, R.; Lankathilaka, K. P. W.; Bornscheuer, U. T.; Liu, D.; Fiedler, A. T.; Holz, R. C.; Bennett, B. Multiple States of Nitrile Hydratase from Rhodococcus equi TG328−2: Structural and Mechanistic Insights from Electron Paramagnetic Resonance and Density Functional Theory Studies. *Biochemistry* **2017**, *56* (24), 3068−3077.

(24) O'Toole, M. G.; Bennett, B.; Mashuta, M. S.; Grapperhaus, C. A. Substrate Binding Preferences and pKa Determinations of a Nitrile Hydratase Model Complex: Variable Solvent Coordination to [(bmmp-TASN)Fe]OTf. 2009, 48, 2300−2308]. *Inorg. Chem.* **2009**, *48*, 2300−2308.

(25) Wang, C.-C.; Lai, Y.-H.; Ou, Y.-M.; Chang, H.-T.; Wang, Y.-S. Critical factors determining the quantification capability of matrix-assisted laser desorption/ionization−time-of-flight mass spectrometry. *Philos. Trans. R. Soc., A* **2016**, *374*, 20150371.

https://doi.org/10.1021/acs.inorgchem.0c02924
Inorg. Chem. 2021, 60, 5432−5435